JCB Report

Homer 2 tunes G protein–coupled receptors stimulus intensity by regulating RGS proteins and PLCβ GAP activities

Dong Min Shin,[1] Marlin Dehoff,[2] Xiang Luo,[4] Shin Hyeok Kang,[2] Jiangchen Tu,[2] Surendra K. Nayak,[5] Elliott M. Ross,[5] Paul F. Worley,[2,3] and Shmuel Muallem[4]

[1]Department of Oral Biology, Brain Korea 21 Project of Medical Sciences, Yonsei University, Seoul 120-752, South Korea
[2]Department of Neuroscience and [3]Department of Neurology/Neurosurgery, Johns Hopkins University School of Medicine, Baltimore, MD 21287
[4]Department of Physiology and [5]Department of Pharmacology, University of Texas Southwestern Medical Center at Dallas, Dallas, TX 75390

Homers are scaffolding proteins that bind G protein–coupled receptors (GPCRs), inositol 1,4,5-triphosphate (IP_3) receptors (IP_3Rs), ryanodine receptors, and TRP channels. However, their role in Ca^{2+} signaling in vivo is not known. Characterization of Ca^{2+} signaling in pancreatic acinar cells from Homer2$^{-/-}$ and Homer3$^{-/-}$ mice showed that Homer 3 has no discernible role in Ca^{2+} signaling in these cells. In contrast, we found that Homer 2 tunes intensity of Ca^{2+} signaling by GPCRs to regulate the frequency of $[Ca^{2+}]_i$ oscillations. Thus, deletion of Homer 2 increased stimulus intensity by increasing the potency for agonists acting on various GPCRs to activate PLCβ and evoke Ca^{2+} release and oscillations. This was not due to aberrant localization of IP_3Rs in cellular microdomains or IP_3R channel activity. Rather, deletion of Homer 2 reduced the effectiveness of exogenous regulators of G proteins signaling proteins (RGS) to inhibit Ca^{2+} signaling in vivo. Moreover, Homer 2 preferentially bound to PLCβ in pancreatic acini and brain extracts and stimulated GAP activity of RGS4 and of PLCβ in an in vitro reconstitution system, with minimal effect on PLCβ-mediated PIP_2 hydrolysis. These findings describe a novel, unexpected function of Homer proteins, demonstrate that RGS proteins and PLCβ GAP activities are regulated functions, and provide a molecular mechanism for tuning signal intensity generated by GPCRs and, thus, the characteristics of $[Ca^{2+}]_i$ oscillations.

Introduction

Receptor-mediated Ca^{2+} signaling consists of a biochemical component that hydrolyzes phosphatidylinositol-bisphosphate (PIP_2)* to generate inositol 1,4,5-triphosphate (IP_3) and a biophysical component that transports Ca^{2+} into and out of the cytosol. In the case of G protein–coupled receptors (GPCRs), the biochemical component is composed of a receptor, the heterotrimeric G protein Gq (and in some cases Gi), and the effector PLCβ. The biophysical component includes the plasma membrane Ca^{2+} ATPase (PMCA) and sarco/endoplasmic reticulum Ca^{2+} ATPase (SERCA) pumps, the IP_3 receptors (IP_3Rs) Ca^{2+} release channels in the ER, and Ca^{2+} influx channels in the PMCA (Berridge, 1993). Ligand binding to GPCRs initiates a well-defined sequence of events resulting in a single transient change in $[Ca^{2+}]_i$ in the case of an intense stimulation, or repetitive $[Ca^{2+}]_i$ oscillations in the case of a weak stimulation (Berridge, 1993). In polarized cells, the Ca^{2+} signal often occurs in the form of highly coordinated and propagating Ca^{2+} waves (Petersen et al., 1994), with receptor-specific initiation sites and propagation patterns (Xu et al., 1996a; Shin et al., 2001).

The highly coordinated $[Ca^{2+}]_i$ oscillations and waves require polarized expression of Ca^{2+}-signaling proteins, their

D.M. Shin, M. Dehoff, and X. Luo contributed equally to this work.

Address correspondence to Shmuel Muallem, Dept. of Physiology, University of Texas Southwestern Medical Center at Dallas, 5323 Harry Hines Blvd., Dallas, TX 75235-9040. Tel.: (214) 648-2593. Fax: (214) 648-8879. E-mail: Shmuel.Muallem@UTSouthwestern.edu; or Paul F. Worley, 600 North Wolfe St., Baltimore, MD 21205. Tel.: (410) 502-5489. Fax: (410) 614-8423. E-mail: pworley@jhmi.edu

*Abbreviations used in this paper: BS, bombesin; CPA, cyclopiazonic acid; GAP, GTPase-activating protein; GPCR, G protein–coupled receptors; IP_3, inositol 1,4,5-triphosphate; IP_3R, IP_3 receptor; pAb, polyclonal antibody; PIP_2, phosphatidylinositol-bisphosphate; PMCA, plasma membrane Ca^{2+} ATPase; RGS, regulators of G proteins signaling; SERCA, sarco/endoplasmic reticulum Ca^{2+} ATPase; SLO, streptolysin O; WT, wild-type.

Key words: Homers; GPCR; Ca^{2+} signaling; regulation; IP_3

organization into complexes, and regulation of each component within the signaling complex. Indeed, Ca^{2+}-signaling proteins are clustered in microdomains of polarized cells, such as the pre- and postsynaptic membranes in neurons (Hering and Sheng, 2001) and the apical pole of secretory cells (Kiselyov et al., 2003). Signaling complexes are assembled with the aid of scaffolding proteins that express multiple protein–protein interacting domains (Hering and Sheng, 2001; Minke and Cook, 2002). The role of scaffolding proteins in tyrosine kinase receptors (Hunter, 2000) and cAMP/PKA-mediated signaling (Smith and Scott, 2002) is well characterized. Much less is known about scaffolding proteins in Ca^{2+} signaling. In synapses, PSD-95, SHANK, GRIP, and probably other scaffolds, participate in assembly of signaling complexes, including Ca^{2+} signaling (Hering and Sheng, 2001). InaD is the scaffold that assembles Ca^{2+}-signaling complexes in *Drosophila* photoreceptors (Minke and Cook, 2002). However, the primary scaffolding protein that assembles Ca^{2+}-signaling complexes in nonneuronal cells is not known. Homer proteins have recently emerged as attractive candidates (Fagni et al., 2002). Homers are scaffolding proteins that are composed of an EVH protein–binding domain, a coiled-coil multimerization domain, and a leucine zipper (Fagni et al., 2002). The EVH domain binds the GPCR mGluR1α/5, IP_3Rs, ryanodine receptors, and probably other proteins involved in Ca^{2+} signaling (Tu et al., 1998; Xiao et al., 1998, 2000). However, the present work reveals that Homers may not function as simple scaffolds, as deletion of Homer 2 or 3 did not disrupt polarized localization of IP_3Rs and other Ca^{2+}-signaling proteins in pancreatic acini, but rather affected the efficiency of signal transduction.

G proteins amplify and transduce signals from the receptor to the appropriate effector, and are, thus, a central regulatory site of signal transduction efficiency. Activation of G proteins involves a receptor-catalyzed GDP-GTP exchange reaction on the α subunit to release Gα·GTP and Gβγ (Gilman, 1987), which, in turn, activate separate effector proteins (Gudermann et al., 1997). The off reaction entails the hydrolysis of GTP and reassembly of the Gα·GDPβγ heterotrimer. This reaction is accelerated by two separate GTPase-activating proteins (GAPs), the PLCβ effector protein (Ross, 1995) and the regulators of G proteins signaling (RGS) proteins (Ross and Wilkie, 2000). In vitro (Ross and Wilkie, 2000) and in vivo studies (Cook et al., 2000) suggest that both catalytic mechanisms participate in Ca^{2+} signaling. Furthermore, regulation of Gαq by RGS proteins confers receptor-specific Ca^{2+} signaling (Xu et al., 1999), drives $[Ca^{2+}]_i$ oscillations (Luo et al., 2001), and probably accounts for the oscillation in $[IP_3]$ during $[Ca^{2+}]_i$ oscillations (Hirose et al., 1999; Nash et al., 2001). $[Ca^{2+}]_i$ oscillations due to $[IP_3]$ oscillations require cyclical activation and inactivation of RGS and/or PLCβ GAP activity. To date, little is known about the regulation of RGS proteins and PLCβ GAP activity.

The results reported here show that Homer 3 does not have a major role in Ca^{2+} signaling in pancreatic acinar cells, whereas Homer 2 regulates GAP activity of both RGS proteins and PLCβ. Deletion of Homer 2 resulted in increased potency of agonist-stimulated Ca^{2+} signaling and, thus, increased frequency of agonist-evoked $[Ca^{2+}]_i$ oscillations. This phenotype was traced to reduced GAP activity of exogenous RGS proteins to inhibit Ca^{2+} signaling in cells from Homer2$^{-/-}$ mice. In support of this mechanism, Homer 2 preferentially binds to PLCβ and activates RGS4 and PLCβ GAP activity in an in vitro reconstitution system. Thus, Homer 2 tunes the intensity of Ca^{2+} signaling to regulate $[Ca^{2+}]_i$ oscillation frequency and, thus, cell functions regulated by this signaling pathway.

Results

Homer proteins are encoded by three genes, *Homer 1*, *2*, and *3* (Xiao et al., 2000; Fagni et al., 2002). Involvement of Homers in Ca^{2+} signaling was concluded from binding of GPCRs and IP_3Rs to the EVH domain of Homer and the partial inhibition of Ca^{2+} signaling in neurons by expression of Homer 1a, a natural dominant negative of Homer scaffolding function (Tu et al., 1998). Based on these observations, it is generally assumed that Homers function as scaffolds that assemble and retain Ca^{2+}-signaling complexes in cellular microdomains (Hering and Sheng, 2001; Fagni et al., 2002). To probe the role of Homers in Ca^{2+} signaling more directly, we generated mice deficient in specific Homer isoforms and characterized Ca^{2+} signaling in cells from these mice. We focused on pancreatic acinar cells because these polarized cells express all Ca^{2+}-signaling proteins in a highly polarized manner at the apical pole (Lee et al., 1997a,b) and generate Ca^{2+} signals in the form of propagating Ca^{2+} waves (Kasai et al., 1993; Shin et al., 2001).

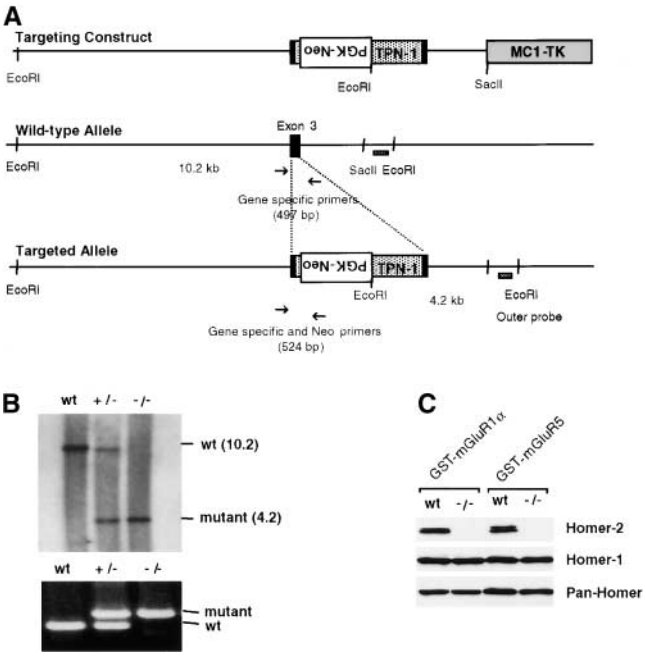

Figure 1. **Deletion of the *homer 2* gene.** (Panel A) Strategy for *homer 2* gene disruption. Transprimer was placed in exon 3 and PGK-neo cassette was inserted in opposite orientation. (B) Genotyping of mice by Southern blot (top) and PCR (bottom). (C) GST pull-down with group I mGluRs.

Deletion of Homers does not affect polarized expression of IP_3Rs

The most basic function of a scaffolding protein is targeting and retention of its binding partners in a defined microdomain. Therefore, we first compared localization and expression of the Homers and IP_3Rs in cells from wild-type (WT) and mutant mice. Fig. 1 describes the generation of the Homer $2^{-/-}$ mice and shows that the gene was deleted (B), and the mRNA (B) and protein (C) could not be detected. Fig. 2 illustrates the localization of the three Homer isoforms and of IP_3Rs in cells from WT and Homer2$^{-/-}$ mice. It is evident that Homers 1 and 2 are expressed exclusively in the apical pole of pancreatic acinar cells (Fig. 2, A–D), the site enriched in all three isoforms of IP_3Rs (Fig. 2, G–L) and other Ca^{2+}-signaling proteins (Lee et al., 1997a,b; Shin et al., 2001; Zhao et al., 2001) and from which Ca^{2+} waves emanate (Xu et al., 1996a; Shin et al., 2001). On the other hand, Homer 3 is expressed in the basal pole (Fig. 2, E and F). Deletion of Homer 2 did not affect expression of Homer 1 or 3. Most notably, deletion of Homer 2 had no effect on the localization of any IP_3R isoform. This was probably not due to the compensatory effect of other Homers because preliminary experiments with pancreatic acini from one mouse from which Homers 1, 2, and 3 were deleted showed no obvious effect of Homers deletion on IP_3Rs localization. This was unexpected in view of the binding of IP_3Rs to the EVH domain of Homers (Tu et al., 1998).

Next, we examined whether deletion of Homer 2 affected expression of the Ca^{2+} transporters that generate the Ca^{2+} signal (Fig. 3). Although all proteins could be detected, attempts to quantify protein expression by Western blot using membranes prepared from pancreatic acini were largely unsuccessful due to excessive protein degradation. As reported before, this was particularly the case for all IP_3Rs (Lee et al., 1997b). Reliable results could be obtained only for SERCA2b, the expression level of which increased 2.2-fold in pancreatic acinar cells from Homer 2-deficient mice (Fig. 3 A). Similar results were obtained with parotid gland (not depicted) and brain membranes (Fig. 3 B). The immunolocalization in Fig. 2 suggests that deletion of Homer 2 has minimal or no effect on expression of all IP_3R isoforms. This was further tested in brain extracts. For the most part, the levels of IP_3Rs were unaffected, although a slight increase in IP_3R1 may have occurred in Homer2$^{-/-}$ cells (Fig. 3, C and D). Similarly, expression of PMCA was unaltered in Homer2$^{-/-}$ cells (Fig. 3 E). These findings imply that the expression and retention of IP_3Rs in cellular microdomains do not require the expression of Homer 2. This conclusion can probably be extended to other components of the Ca^{2+}-signaling complex.

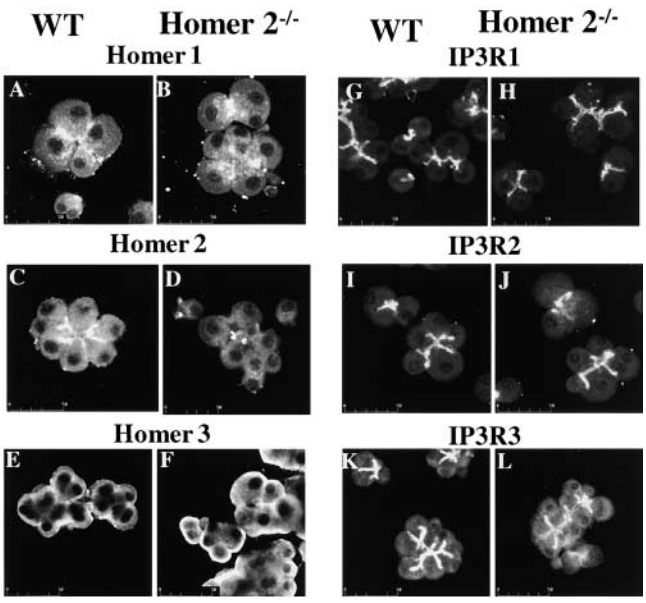

Figure 2. **Localization of Homer proteins and IP_3Rs in WT and Homer $2^{-/-}$ cells.** Acini from WT and Homer $2^{-/-}$ mice were stained for (A and B) Homer 1, (C and D) Homer 2, (E and F) Homer 3, (G and H) IP_3R, (I and J) IP_3R2, and (K and L) IP_3R3. Note lack of effect of Homer 2 deletion on expression and localization of the other Homers and, in particular, IP_3Rs.

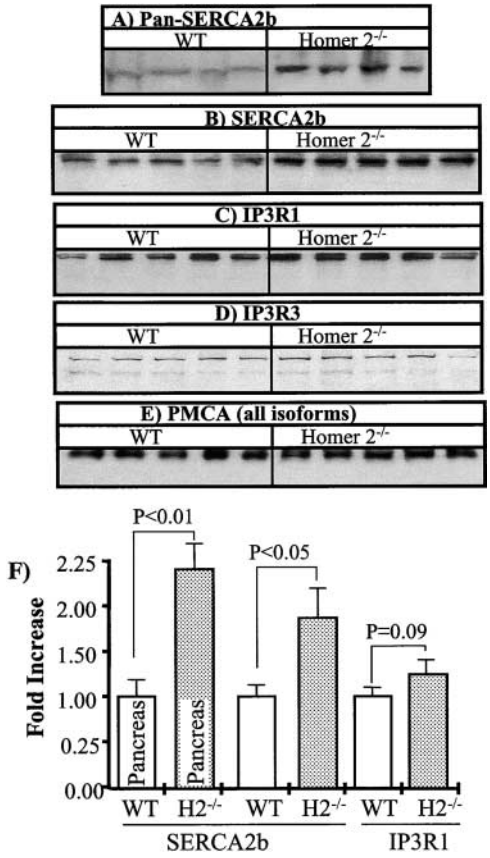

Figure 3. **Expression of Ca^{2+} transporters in WT and Homer $2^{-/-}$ cells.** (A) The level of SERCA2b was analyzed in extracts prepared from pancreatic acini of four WT and four Homer $2^{-/-}$ mice. Extracts prepared from the brain of five WT and five Homer $2^{-/-}$ mice were also used to analyze the levels of (B) SERCA2b, (C) IP_3R1, (D) IP_3R3, and (E) PMCA. Expression was analyzed by densitometry and was unaltered for all Ca^{2+} transporters, except (F) SERCA2b. The results in F are expressed as the mean ± SEM.

Homer 3 does not participate in Ca^{2+} signaling in secretory acinar cells

Expression of Homer 3 at the basal pole of pancreatic acinar cells, its absence from the apical pole, and the specificity of

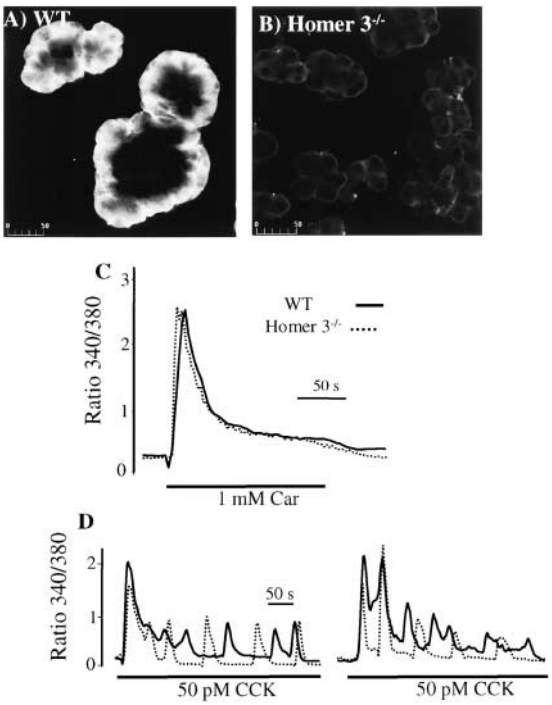

Figure 4. **Ca^{2+} signaling in cells from Homer $3^{-/-}$ mice.** A and B show immunolocalization of Homer 3 in WT and Homer $3^{-/-}$ cells, respectively. Examples of the Ca^{2+} response of WT (bold lines) or Homer $3^{-/-}$ cells (dashed lines) to stimulation with (C) 1 mM carbachol or (D) 50 pM CCK is shown. The traces in D are with acini from two separate mice. Similar results were obtained using various protocols with cells prepared from nine WT and nine Homer $3^{-/-}$ mice.

Homer 3 localization is further illustrated in Fig. 4 (A and B). A comparison of Ca^{2+} signals obtained in WT and Homer $3^{-/-}$ cells stimulated with high agonist concentration to trigger a single $[Ca^{2+}]_i$ transient (Fig. 4 C) or stimulated with low agonist concentration to evoke $[Ca^{2+}]_i$ oscillations (Fig. 4 D) revealed no clear difference in any parameter of the Ca^{2+} signals. Likewise, no differences were observed in the Ca^{2+} signals recorded from WT and Homer $3^{-/-}$ cells using the protocols in Figs. 4 and 5. Deletion of Homer 3 also had no effect on localization of Ca^{2+}-signaling proteins in the apical pole of pancreatic, submandibular, and parotid gland acinar and duct cells, as was found for Homer $2^{-/-}$ (unpublished data). Hence, it appears that Homer 3 does not participate directly in controlling GPCR-dependent Ca^{2+} signaling in the cells and tissue types examined. This is not surprising considering the differential localization of Ca^{2+}-signaling complexes and Homer 3. The role of Homer 3 in cell function remains to be defined. Preliminary experiments with cells from Homer1$^{-/-}$ mice showed that deletion of Homer 1 did not affect agonist-stimulated IP_3 production or Ca^{2+} mobilization in pancreatic acini (unpublished data), a phenotype different from that of cells from Homer $2^{-/-}$ mice.

Deletion of Homer 2 increases potency of agonist stimulation

A different picture emerged when Ca^{2+} signaling was analyzed in cells from Homer2$^{-/-}$ mice. The effect of Homer 2 deletion on Ca^{2+} signaling was first studied in maximally stimulated WT and Homer2$^{-/-}$ acinar cells. Fig. 5 A and the summary in Fig. 5 C show that 1 mM carbachol increased $[Ca^{2+}]_i$ to a higher level in Homer2$^{-/-}$ cells. In addition, Homer2$^{-/-}$ cells stimulated with carbachol reduced $[Ca^{2+}]_i$ to a stable plateau faster than cells from WT mice. However, the plateau level was similar in both cell types. The higher $[Ca^{2+}]_i$ increase in Homer2$^{-/-}$ cells could be due to increased Ca^{2+} release from internal stores and/or increased Ca^{2+} influx across the PMCA. To determine the contribution of each pathway we compared Ca^{2+} influx in the two cell types by a Ca^{2+}-removal and -readdition protocol in stimulated cells. The cells were also treated with the SERCA pump inhibitor cyclopiazonic acid (CPA) to maximally deplete the stores and activate Ca^{2+} entry. Fig. 5 A (inset) shows that deletion of Homer 2 had no effect on Ca^{2+} influx. Similar results were observed in all seven similar experiments. Furthermore, removal of Ca^{2+} from the medium and stimulation with carbachol and CPA did not reduce the difference in $[Ca^{2+}]_i$ increase between the two cell types (Fig. 5 C, middle columns, results summary). This indicates a higher Ca^{2+} load of the ER of Homer2$^{-/-}$ cells, as expected from the increased expression of SERCA2b demonstrated in Fig. 3. Therefore, the higher increase in $[Ca^{2+}]_i$ in Homer2$^{-/-}$ cells is due to increased Ca^{2+} release from internal stores. The faster rate of $[Ca^{2+}]_i$ decrease after Ca^{2+} release can be due to faster pumping of the Ca^{2+} out of the cells by PMCA or due to faster clearance of cytosolic Ca^{2+} by SERCA pumps. This was addressed by inhibiting SERCA pump activity at the onset of cell stimulation. Fig. 5 B shows that under these conditions $[Ca^{2+}]_i$ was still increased to a higher level in Homer2$^{-/-}$ cells, but now the rate of $[Ca^{2+}]_i$ reduction was similar in WT and Homer2$^{-/-}$ cells. In summary, the observed altered properties of the Ca^{2+} signal in maximally stimulated Homer2$^{-/-}$ cells is precisely what is expected from the adaptive increased expression of SERCA2b shown in Fig. 3.

To probe Ca^{2+} signaling further, we examined the response to increasing concentrations of carbachol. At low concentrations, agonists evoke $[Ca^{2+}]_i$ oscillations. The frequency, and in some cases, the amplitude, of the oscillations increases with increased agonist concentration until at a high enough agonist concentration the oscillations merge into a single transient increase in $[Ca^{2+}]_i$ (Berridge, 1993). This pattern is shown in Fig. 5 (D–F), left traces, for cells from WT mice. At 1 μM, carbachol induced low frequency oscillations (see Fig. 6 B for summary). The residual Ca^{2+} content in the stores was estimated by discharging it by exposing the cells to 1 mM carbachol and 10 μM CPA. 2.5 μM carbachol caused a substantial initial increase in $[Ca^{2+}]_i$ that was followed by high frequency–low amplitude oscillations. Finally, 10 μM carbachol evoked a large increase in $[Ca^{2+}]_i$ with high frequency oscillations superimposed on the downward stroke of $[Ca^{2+}]_i$. 10 μM carbachol released ~70% of stored Ca^{2+}. Remarkably, deletion of Homer 2 increased the response at all carbachol concentrations between 1 and 10 μM. Thus, 1 μM carbachol induced a response in Homer2$^{-/-}$ cells similar to that induced by 2.5 μM carbachol in WT cells. 2.5 μM carbachol caused a transient increase in $[Ca^{2+}]_i$ while releasing ~60% of stored Ca^{2+},

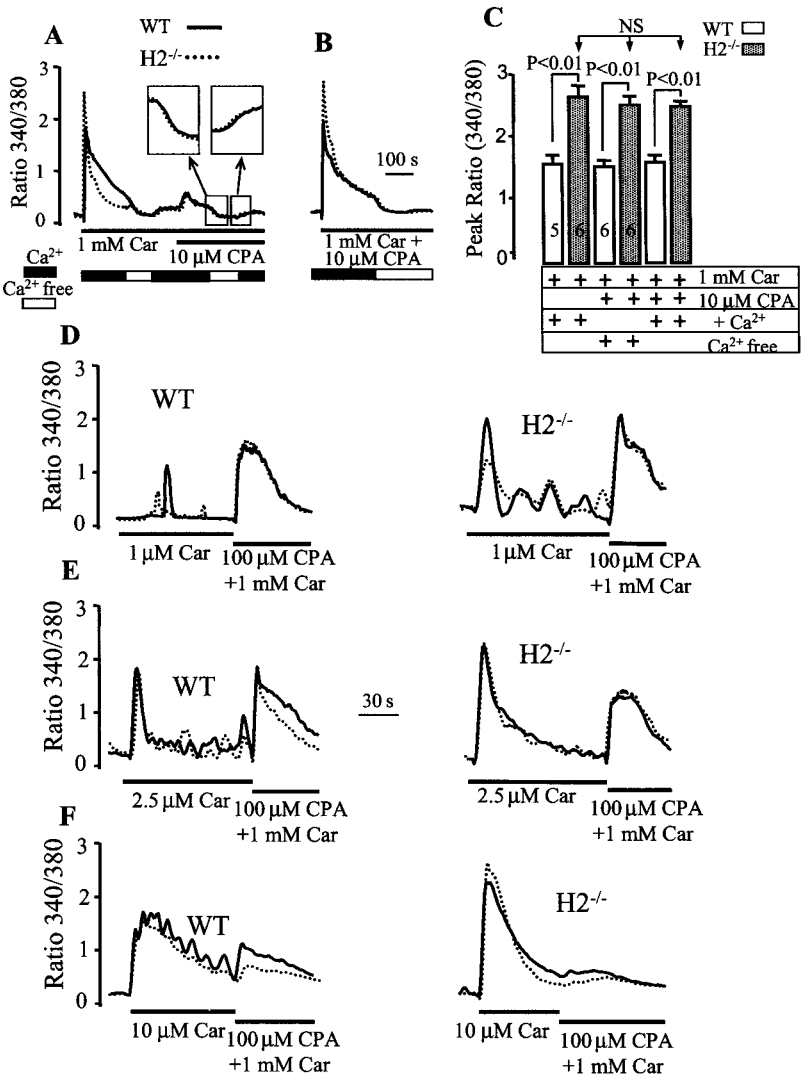

Figure 5. **Characterization of Ca^{2+} signaling in Homer $2^{-/-}$ cells.** (A and B) Cells from WT (solid lines) and Homer $2^{-/-}$ (dashed lines) mice were used to measure the $[Ca^{2+}]_i$ response to stimulation with 1 mM carbachol in the presence (black bars) or absence (open bars) of (A) 2 mM medium Ca^{2+}. Where indicated by the bold lines, the cells were also treated with 10 μM CPA to inhibit the SERCA pumps. C shows the mean ± SEM of the indicated number of experiments performed with cells from different mice. D–F compare the responses obtained with WT (left) and Homer $2^{-/-}$ (right) cells stimulated with (D) 1, (E) 2.5, or (F) 10 μM carbachol. The residual Ca^{2+} pool after each stimulation was estimated by completely discharging it with 1 mM carbachol and 100 μM CPA. Each panel shows two traces from two cells present in the same recording field. Similar results were obtained with cells prepared from three different mice of each phenotype.

whereas 10 μM carbachol mobilized the entire intracellular Ca^{2+} pool of Homer2$^{-/-}$ cells, similar to the effect of 100 μM carbachol in WT cells.

Deletion of Homer 2 increased the potency of all Gq-coupled receptors expressed in acinar cells examined. Fig. 6 shows part of the results obtained with bombesin (BS) and CCK stimulation, focusing on the physiological response of $[Ca^{2+}]_i$ oscillations. CCK at 20 pM induced typical baseline $[Ca^{2+}]_i$ oscillations in cells from WT mice. The $[Ca^{2+}]_i$ oscillations evoked by the same concentration of CCK in cells from Homer2$^{-/-}$ mice occurred at a frequency about twice as higher than those recorded in cells from WT mice (Fig. 6, A and B). The traces in Fig. 6 C show that increasing BS concentration from 50 to 100 pM increased the frequency of the oscillations by 1.7-fold in WT cells. The same fold increase in frequency (1.8) was observed in Homer2$^{-/-}$ cells, but at each BS concentration, the frequency of the oscillations was ∼2.3-fold higher in Homer2$^{-/-}$ cells. In aggregate, the results of Figs. 5 and 6 show that deletion of Homer 2 increases the potency of agonists to stimulate Ca^{2+} signaling by GPCRs. The increase in potency is due to a change in a regulatory step common to signaling by GPCRs because the response evoked by all GPCRs examined was affected. In the next stage, we searched for this Homer 2–regulated general mechanism.

Homer 2 does not affect IP_3-mediated Ca^{2+} release

The frequency of Ca^{2+} oscillations is controlled by a biochemical mechanism through the production of IP_3 (Luo et al., 2001) and by several biophysical mechanisms that control the activity of the IP_3Rs (Kiselyov et al., 2003). The activity of IP_3Rs is regulated by the concentrations of IP_3 and $[Ca^{2+}]_i$ (Thrower et al., 2001), as well as Ca^{2+} content in the stores, which increases channel sensitivity to IP_3 (Missiaen et al., 1992; Xu et al., 1996b). Because of the increased SERCA2b and Ca^{2+} content in the stores of Homer2$^{-/-}$ cells, we considered the possibility that Ca^{2+} release from the stores of these cells was more sensitive to IP_3, leading to increased frequency of $[Ca^{2+}]_i$ oscillations. The results in Fig. 7 exclude this possibility. Fig. 7 (A–C) shows the same potency for IP_3 to release Ca^{2+} from the stores of streptolysin O (SLO)–permeabilized WT and Homer2$^{-/-}$ cells. In Fig. 7 (D–H), the frequency of IP_3-evoked $[Ca^{2+}]_i$ oscillations was measured in intact cells. In these experiments, the whole cell mode of the patch clamp technique was used to record the Ca^{2+}-activated Cl^- current as a reporter of

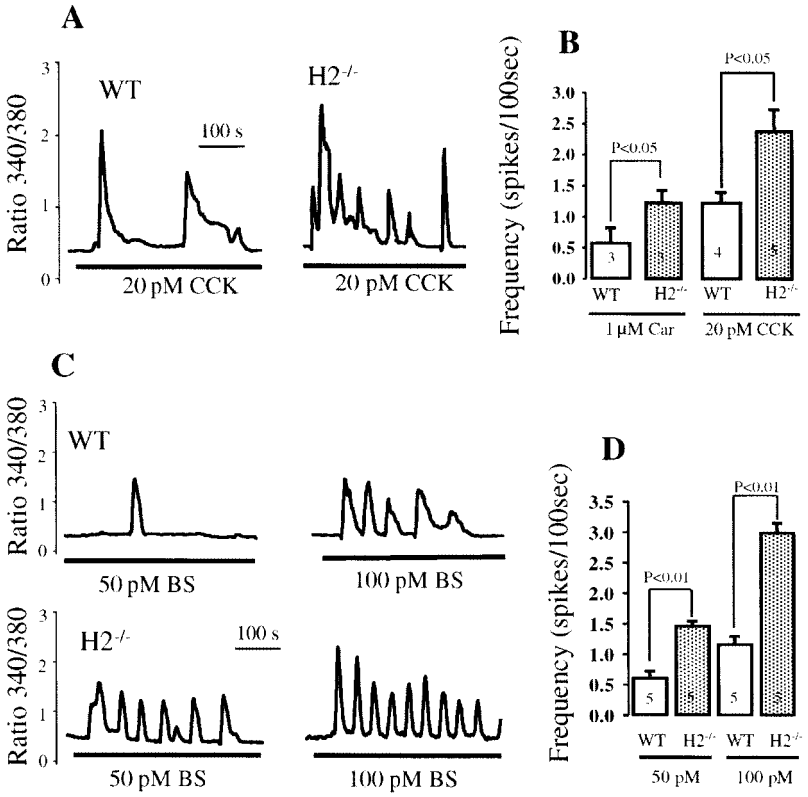

Figure 6. **Agonist-evoked $[Ca^{2+}]_i$ oscillations in WT and Homer $2^{-/-}$ cells.** As indicated in the figure, cells from WT and Homer $2^{-/-}$ mice were stimulated with (A) 20 pM CCK, or (C) 50 and 100 pM BS to measure $[Ca^{2+}]_i$ oscillations. The frequency of the oscillations, determined in cells prepared from three to five mice as indicated in the figure, are summarized in B for 1 μM carbachol and 20 pM CCK, and in D for the two concentrations of BS, and are given as the mean ± SEM.

$[Ca^{2+}]_i$ (Zeng et al., 1996). The controls in Fig. 7 (D and F) show that $[Ca^{2+}]_i$ oscillations evoked by 0.5 μM carbachol occurred at a higher frequency (1.86- ± 0.26-fold, $n = 7$) in Homer2$^{-/-}$ compared with control cells, whereas the response to maximal agonist stimulation was the same in both cell types. Long-lasting, IP_3-evoked $[Ca^{2+}]_i$ oscillations were induced by infusing the cells with 20 μM of the nonhydrolyzable IP_3 analogue, 2,4,5 IP_3. Fig. 7 (E–G) shows that IP_3 evoked $[Ca^{2+}]_i$ oscillations with indistinguishable frequency in the two cell types. The implications of the findings in Fig. 7 are that the function of the IP_3Rs is the same in cells from WT and Homer2$^{-/-}$ mice and that the increased GPCR sensitivity to agonist stimulation in Homer2$^{-/-}$ cells is due to regulation by Homer 2 of a step upstream of Ca^{2+} release by IP_3.

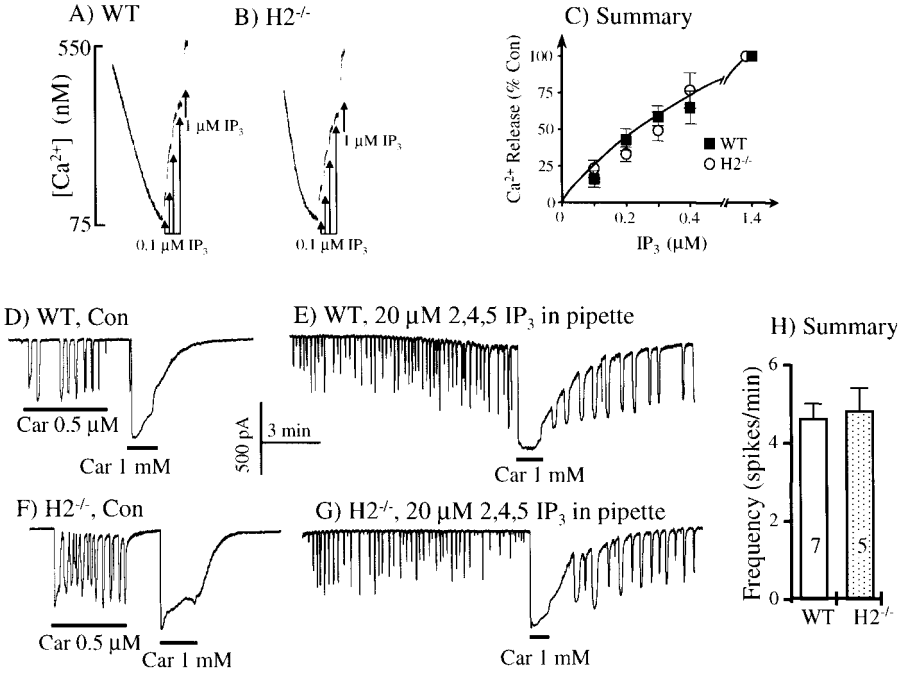

Figure 7. **IP_3-mediated Ca^{2+} release from WT and Homer $2^{-/-}$ cells.** Cells from (A) WT and (B) Homer $2^{-/-}$ mice were permeabilized with SLO and allowed to reduce $[Ca^{2+}]$ of the incubation medium to ~75 nM. Next, Ca^{2+} release was measured by adding increasing concentrations of IP_3 (A and B, arrows). C summarizes the results obtained in five experiments with cells prepared from three WT and three Homer2$^{-/-}$ mice. The results are expressed as the mean ± SEM. In D–H, cells from (D and E) WT and (F and G) Homer $2^{-/-}$ were used to record the Ca^{2+}-activated Cl^- current using whole cell recording. In E and G, the pipette solution also contained 20 μM 2,4,5 IP_3. Where indicated by the bars, the cells were stimulated with (D and F) 0.5 μM or (D–G) 1 mM carbachol. H presents the mean ± SEM of the frequency of IP_3-evoked $[Ca^{2+}]_i$ oscillations in seven experiments with WT cells obtained from three mice and five experiments with Homer $2^{-/-}$ cells obtained from two mice.

Homer 2 regulates RGS proteins and PLCβ GAP activities

Enhanced activity of the biochemical component of Ca^{2+} signaling in Homer2$^{-/-}$ cells implies enhanced activation of PLCβ and IP_3 production, which can account for the increased signal intensity and frequency of Ca^{2+} oscillations. This was tested by measuring the dose response for carbachol-stimulated IP_3 production. Notably, Fig. 8 A shows that deletion of Homer 2 increased the potency of carbachol in stimulating IP_3 production about fivefold without affecting maximally stimulated IP_3 production. The same phenomenon was observed using two submaximal and one maximal concentration of CCK and BS (unpublished data).

IP_3 production entails activation of Gq by receptors and activation of PLCβ by Gαq. The steady-state level of active Gαq is determined by the balance between the receptor-catalyzed GTP-GDP exchange reaction on Gαq and hydrolysis of GTP by Gαq (Gilman, 1987). GTP hydrolysis is accelerated by RGS proteins (Ross and Wilkie, 2000) and by the effector itself, PLCβ (Ross, 1995). The increased potency of agonists in Homer2$^{-/-}$ cells could be due to increased activation of PLCβ by Gαq-GTP, stimulation of the receptor catalyzed GTP-GDP exchange reaction, inhibition of the GAP activity of RGS proteins and PLCβ, or any combination of the above. The first possibility was tested by measuring the dose response for activation of PLCβ by GTPγS. Fig. 8 B shows that activation of PLCβ by GTPγS (activated Gαq) was the same in WT and Homer2$^{-/-}$ cells. Hence, deletion of Homer 2 did not affect activation of PLCβ by Gαq.

To test the second possibility, we measured the inhibition of Ca^{2+} signaling by RGS4, which was infused into the cells using a patch pipette. Due to expression of several RGS proteins in one cell and the lack of information as to the specific RGS protein in each Ca^{2+}-signaling complex, it was not possible to manipulate the native RGS proteins activity. Instead, we measured the ability of exogenous RGS4 to inhibit Ca^{2+} signaling. Fig. 9 (A–C) shows that in WT cells, 0.25 nM RGS4 abolished $[Ca^{2+}]_i$ oscillations in response to 0.5 μM carbachol and inhibited >90% of the response to maximal stimulation with 1 mM carbachol. In contrast, in Homer2$^{-/-}$ cells, 0.25 nM RGS4 only partially inhibited the response to maximal carbachol stimulation (Fig. 9 E). The response to 1 mM carbachol was partially blocked by up to 1 nM RGS4 (Fig. 9 F), which converted the sustained response to $[Ca^{2+}]_i$ oscillations. Complete inhibition of the

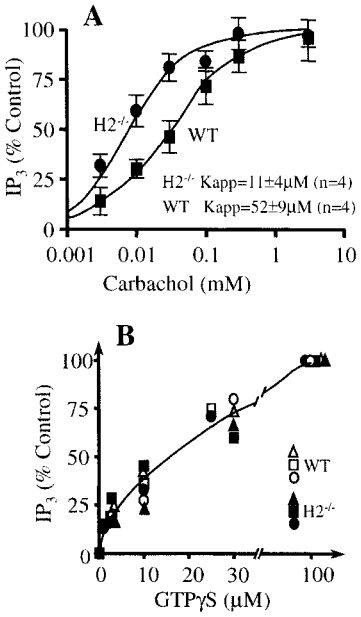

Figure 8. **PLCβ activity in agonist and GTPγS stimulated cells from WT and Homer 2$^{-/-}$ cells.** (A) Intact cells from WT (squares) or Homer 2$^{-/-}$ (circles) mice were stimulated with various [carbachol] for 5 s, the reactions were stopped, and IP_3 was extracted and measured as described in Materials and methods. The figure shows the mean ± SEM of four experiments performed in duplicates with four different cell preparations. (B) Cells from three WT (open symbols) and three Homer 2$^{-/-}$ mice (closed symbols) were permeabilized with SLO in intracellular-like medium and stimulated with the indicated [GTPγS] for 15 s at 37°C. This procedure requires a large amount of cells to ensure reduction of medium $[Ca^{2+}]$ to the nanometer range (Fig. 7) and, therefore, single determinations were performed at each [GTPγS]. Different symbols represent experiments with different cell preparations. The same open and closed symbols indicate experiments performed in parallel with cells from WT and Homer 2$^{-/-}$ mice.

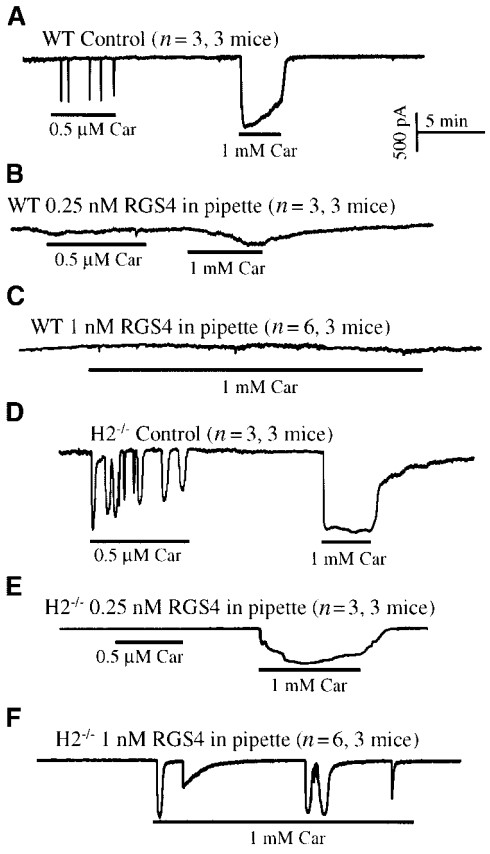

Figure 9. **Effect of RGS4 on Ca^{2+} signaling in WT and Homer 2$^{-/-}$ cells.** Cells from (A–C) WT or (D–F) Homer 2$^{-/-}$ mice were infused with (A and D) a control pipette solution, or pipette solutions containing (B and E) 0.25 nM or (C and F) 1 nM RGS4. About 7 min after brake-in to allow equilibration of RGS4 between pipette solution and cytosol, the cells were stimulated with 0.5 μM or 1 mM carbachol, as indicated by the bars. The number of experiments performed with similar results is indicated in parenthesis next to each trace.

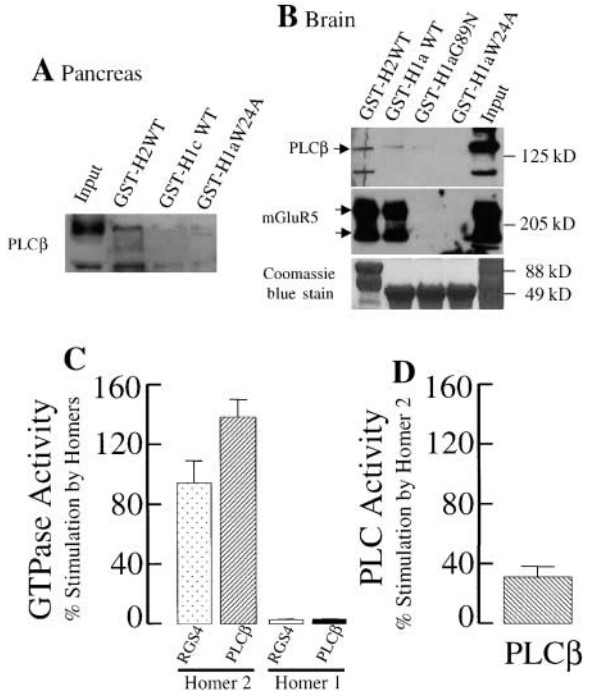

Figure 10. **Interaction of Homers with PLCβ and effect of Homer 2 on RGS4 and PLCβ GAP activity and PLCβ PIP_2 hydrolytic activity in a phospholipid reconstitution system.** (A and B) Soluble lysates from (A) pancreatic acini or (B) adult rat forebrain were assayed for binding to GST-Homer fusion proteins. (A) Homer 2, but not Homer 1c and the mutant Homer 1aW24A, binds PLCβ. (B, top) PLCβ binds full-length Homer 2 preferentially to WT Homer 1 EVH domain or to the Homer 1 mutants W24A and G89N. Input lanes are 10% of that used for the binding assay. (Middle) mGluR5 binds strongly to both Homer 2 and WT Homer 1, but not to the mutants. (Bottom) Coomassie stain of gel showing GST proteins. (C and D) Recombinant, purified M1 receptor, and Gαβγ heterotrimer were reconstituted into liposomes containing PIP_2 and used for measurements of (C) GTPase activity or (D) PIP_2 hydrolysis. GTPase activity was measured in the absence and presence of 2–5 nM RGS4 or 2 nM PLCβ, and in the absence and presence of 250 nM Homer 2 or 1. GTPase activity was initiated by stimulation with 1 mM carbachol. C shows the results of six experiments with RGS4, four experiments with PLCβ performed in duplicate with two separate batches of Homer 2, and two experiments performed in duplicate with Homer 1 and RGS4 or PLCβ. The proteoliposomes were also used to assay PLCβ activity by measuring hydrolysis of (D) PIP_2. The results in D are from seven experiments performed in duplicates and with two batches of Homer 2. Stimulation by Homer 2 was calculated as a percentage of the activity measured in the absence of Homers 1 and 2 and the presence of RGS4 or PLCβ. GAP activity in the absence of Homer 2 and the presence of RGS4 or PLCβ averaged 4.62 ± 0.7 ($n = 9$) and 4.16 ± 0.34 ($n = 7$) pmol Pi released/min/pmol Gq, respectively. Basal PLC PIP_2 hydrolytic activity averaged 2.01 ± 0.12 ($n = 10$) pmol IP_3 released/min/pmol PLCβ. The results are expressed as the mean ± SEM.

response to 1 mM carbachol in Homer2$^{-/-}$ cells was observed at RGS4 concentrations above 2.5 nM ($n = 4$).

To corroborate this unexpected consequence of Homer 2 deletion, we measured the effect of recombinant Homer 2 on the GAP activity of RGS4 in an in vitro reconstitution system. The reconstitution system included the M1 muscarinic receptor and the heterotrimer Gαqβγ reconstituted into liposomes (Biddlecome et al., 1996). The Gαq GTPase activity in this system is dependent on receptor stimulation by carbachol and is inhibited by the muscarinic receptor antagonist atropine (Zeng et al., 1998). Fig. 10 C shows that Homer 2 increased RGS4 GAP activity by ~90%. Importantly, stimulation of RGS4 GAP activity was specific to Homer 2, as Homer 1 had no effect.

PLCβ also functions as a Gα GAP (Cook et al., 2000). Because of the PIP_2 hydrolyzing activity of PLCβ, it is not presently feasible to evaluate the significance of PLCβ GAP in vivo. However, to test the possibility that PLCβ GAP contributes to the enhanced signaling in Homer2$^{-/-}$ cells, we examined if Homers associate with PLCβ in vivo. For this we used GST-Homer 2, GST-Homer 1a and 1c, and two GST-Homer 1a mutants whose EVH domains were unable to bind PLCβ. Fig. 10 A shows that Homer 2 bound PLCβ in pancreatic acinar cell extract better than Homer 1c, and that Homer-PLCβ binding was inhibited by point mutations in the EVH domain. This point mutation destroys binding of all Homer isoforms. The general applicability of these findings is demonstrated by showing a similar profile of Homer-PLCβ binding in brain extract (Fig. 10 B). Homers 1 and 2 bound a comparable amount of mGluR5 monomers and dimers from the same brain extract, and this binding was abolished by the mutations in the EVH domain. The same experiment could not be done with RGS proteins due to a lack of antibodies with sufficient affinity to detect the low level of native RGS proteins.

The preferential binding of PLCβ to signaling complexes containing Homer 2 prompted us to test the effect of Homer 2 on PLCβ-GAP activity in the in vitro reconstitution system. Fig. 10 (C and D) shows the effect of Homer 2 on both PLCβ GAP activity and PIP_2 hydrolysis. Homer 2 stimulated PLCβ GAP activity by ~140%. This was better than Homer 2 stimulation of RGS4 GAP activity. Like RGS4 stimulation, PLCβ stimulation was specific for Homer 2; Homer 1 had no effect on PLCβ GAP activity. Homer 2 stimulated PLCβ PIP_2 hydrolytic activity by only 35%. Homer 2 regulation of RGS4 and PLCβ GAP explains at least in part the effect of Homer 2 deletion on Ca^{2+} signaling.

Discussion

The findings in the present work reveal several unexpected novel functions of Homer proteins and clarify the role of Homer 2 in Ca^{2+} signaling. The first finding of note is that expression of Homer proteins is isoform specific. Homer 3 is expressed in the basal pole, whereas Homers 1 and 2 are restricted to the apical pole. This already indicates that Homers must have nonoverlapping cellular functions. Indeed, Homer 3 has no discernible function in Ca^{2+} signaling in pancreatic acinar cells. Second, based on the modular structure of Homer proteins (EVH and C-C domains and a leucine zipper; Fagni et al., 2002) and their ability to bind the GPCR mGlu5 and IP_3Rs (Tu et al., 1998), it is generally assumed that Homer proteins act as scaffolding proteins to assemble Ca^{2+}-signaling complexes in cellular microdomains (Hering and Sheng, 2001; Fagni et al., 2002). Our results show that this is not the case for either Homer 2 or 3. Thus, deletion of these Homers (and of all Homers together) does not affect localization or expression of any IP_3R isoform.

The only effect observed is increased SERCA2b protein and activity in Homer2$^{-/-}$ cells. This is probably due to an adaptive response of the Ca^{2+}-signaling system to the increased responsiveness of Homer2$^{-/-}$ cells to agonist stimulation. Several previous papers in heterologous systems (Liu et al., 1996; Brini et al., 2000) and in vivo (Zhao et al., 2001) have shown translational adaptation of the Ca^{2+}-transporting machinery to disturbances in expression of Ca^{2+}-transporting proteins.

The most notable finding in the present work is that Homer 2 functions to tune the intensity of agonist stimulation through regulation of RGS proteins and PLCβ GAP activities. Thus, deletion of Homer 2 left-shift the dose response for agonist-stimulated IP_3 production and Ca^{2+} signaling without affecting the activation of PLCβ by activated Gα, while reducing the effectiveness of exogenous RGS proteins to inhibit Ca^{2+} signaling in vivo. These findings were corroborated by demonstrating direct activation of RGS proteins and PLCβ GAP activities in reconstitution system with recombinant proteins. The physiological significance of these findings is demonstrated by the nearly twofold increased frequency of $[Ca^{2+}]_i$ oscillations in Homer2$^{-/-}$ cells.

In a previous work, we showed that RGS proteins provide a biochemical control of $[Ca^{2+}]_i$ oscillations (Luo et al., 2001), thus, providing a molecular mechanism for oscillatory changes in $[IP_3]$ (Hirose et al., 1999; Nash et al., 2001) to drive $[Ca^{2+}]_i$ oscillations. This mechanism explicitly implies that the activity of RGS proteins oscillates to induce oscillations in $[IP_3]$ and, consequently, $[Ca^{2+}]_i$ oscillations (Luo et al., 2001). How the activity of RGS proteins is regulated during $[Ca^{2+}]_i$ oscillations remains unclear. Here, we show that Homer 2 can regulate this activity in vivo and in vitro. Furthermore, we show that PLCβ GAP activity is not fixed, but is also regulated by Homer 2. Based on these findings, we propose that Homer 2 participates in regulating the GTPase reaction in the G protein turnover cycle to tune stimulus intensity.

At present, it is not clear how Homer 2 regulates RGS proteins and PLCβ GAP activities. However, the findings that Homer 2 preferentially binds PLCβ in pancreatic and brain extracts, that stimulation of GAP activity by Homer 2 can be reproduced in the minimal in vitro system, that Homer 2 activates GAP activity of two very different proteins whose only common feature is that they can bind to Gαq, and that Homer 2 has protein–protein binding domains all suggest that Homer 2 may control the proximity of the GAPs to Gαq and, thus, the efficiency of the GTPase reaction. This possibility and the molecular details of how Homer 2 controls GAP activity in vivo remain to be determined.

Regulation of RGS proteins and PLCβ GAP activities by Homer 2 raises the question of the significance of Homer binding to GPCRs and IP_3Rs in Ca^{2+} signaling. Binding of Homer 2 or any of the Homers to one protein does not exclude binding and regulation of other proteins within the Ca^{2+}-signaling complex. A more intriguing possibility is that different Homer isoforms mediate each of the interactions. In either case, it is clear that although Homer proteins do not appear to be the central scaffolding proteins that assemble the Ca^{2+}-signaling complexes, they play an essential role in controlling Ca^{2+} signaling. One of their central roles is tuning Ca^{2+}-signaling intensity. By tuning signal intensity, Homer 2 determines the frequency of $[Ca^{2+}]_i$ oscillations and, in this way, controls the many cellular functions regulated by $[Ca^{2+}]_i$ oscillations (Carafoli, 2002).

Materials and methods

Materials

Cyclopiazonic acid, 1,4,5 and 2,4,5 IP_3 were purchased from Qbiogene. The antibodies used in the present work were obtained from the following sources. Anti-Homer polyclonal antibodies (pAbs), and Homers 1, 2, and 3 were prepared as described previously (Tu et al., 1998). Anti-IP_3R1, 2, and 3 pAbs were a gift from Dr. A. Tanimura (University of Hokkaido, Ishikari-Tobetsu, Japan). Anti-IP_3R3 mAb was purchased from Transduction Laboratories. Anti-PMCA mAb was purchased from Affinity BioReagents, Inc. Anti-SERCA2b pAb was a gift from Dr. F. Wuytack (Catholic University of Leuven, Leuven, Belgium). Purified RGS4 and PLCβ were prepared as described previously (Zeng et al., 1998).

Generation of Homer 2 and 3 mutant mice

The *homer 2* targeting construct was generated by inserting transprimer-1 into exon 3 of a 10.2-kb BAC fragment of the mouse *homer 2* gene (Fig. 1). PGK-Neo was cloned into the unique PmeI site, and the resulting vector was subcloned into an MC1-TK vector. The resulting targeting construct was linearized and electroporated into R1 ES cells. Cells were selected with G-418 and gancyclovir. Clones were picked, screened by PCR, and confirmed by Southern blotting for homologous recombination. Clones were injected into blastocysts, and chimeras were mated to C57BL/6 mice to produce Homer 2 heterozygotes that were crossed to generate WT and Homer2$^{-/-}$ mice. Homer3$^{-/-}$ mice were generated using a similar strategy as that used to delete Homer2, except that the PGK-Neo cassette was directly inserted into exon 3 of Homer3 at the SmaI site.

Preparation of pancreatic acini

Acini were prepared from the pancreas of WT, Homer2$^{-/-}$, and Homer3$^{-/-}$ mice by limited collagenase digestion as described previously (Shin et al., 2001). After isolation, the acini were resuspended in a standard solution A ([mM] 140 NaCl, 5 KCl, 1 $MgCl_2$, 1 $CaCl_2$, 10 Hepes, pH 7.4 with NaOH, 10 glucose, and 0.1% BSA), and kept on ice until use. Doublet or triplet acinar cell clusters were obtained by incubating a minced pancreas in a 0.025% trypsin, 0.02% EDTA solution for 5 min at 37°C. After washing with solution A supplemented with 0.02% soybean trypsin inhibitor (PSA), doublets and triplets were liberated by a 7-min incubation at 37°C in the same solution that also contained 160 U/ml pure collagenase. The cells were washed with solution A and kept on ice until use.

Measurement of $[Ca^{2+}]_i$

Cells in PSA were incubated with 5 μM Fura2/AM for 30 min at room temperature and washed once with PSA. Samples of cells were plated on glass coverslips that formed the bottom of a perfusion chamber. After 2–3 min of incubation, to allow cell attachment to the coverslip, the cells were continuously perfused with prewarmed (37°C) solution A at a rate of 5 ml/min (30 vol chamber/min). Agonists were delivered to the cells by inclusion in the perfusate. Fura2 fluorescence was measured at excitation wavelengths of 340 and 380 nm using a PTI image acquisition and analysis system as detailed previously (Shin et al., 2001).

Electrophysiology

The whole cell configuration of the patch clamp technique was used for measurement of Ca^{2+}-activated Cl^- current as a reporter of $[Ca^{2+}]_i$ next to the PMCA. The experiments were performed with single acinar cells perfused with solution A. The standard pipette solution contained (mM): 140 KCl, 1 $MgCl_2$, 0.1 EGTA, 5 ATP, 10 Hepes (pH 7.3 with KOH) with or without 2,4,5 IP_3 or between 0.25 and 10 nM RGS4, as described previously (Zeng et al., 1996). The RGS4 was dialyzed against an ATP-free pipette solution and concentrated to ~5 μM with a centricone system. Seals of 6–10 GΩ were produced on the cell membrane, and the whole cell configuration was obtained by gentle suction or voltage pulses of 0.5 V for 0.3–1 ms. The patch clamp output (Axopatch-1B; Axon Instruments, Inc.) was filtered at 20 Hz. Recording was performed with patch clamp 6.0 and a Digi-Data interface (model 1200; Axon Instruments, Inc.). The current was recorded at a holding potential of −40 mV. The oscillation frequency was determined from a stretch of at least 5 min starting at the first full Ca^{2+} spike. The number of spikes over this time period was counted to determine the number of

spikes/minute and results from at least five cells from two mice were used to obtain the results listed in the text and shown in Fig. 7.

Measurement of Ca^{2+} uptake and release from internal stores

IP_3-mediated Ca^{2+} release from internal stores was measured in SLO-permeabilized cells as described previously (Xu et al., 1996b). In brief, cells washed with a high K^+, Chelex-treated medium were added to the same medium containing an ATP regeneration system (comprised of 3 mM ATP, 5 mM $MgCl_2$, 10 mM creatine phosphate, and 5 U/ml creatine kinase), a cocktail of mitochondrial inhibitors, 2 μM Fluo3 and 3 mg/ml SLO (Difco). In this medium, the cells were almost instantaneously permeabilized so that Ca^{2+} uptake into the ER could be measured immediately. Uptake of Ca^{2+} into the ER was allowed to continue until medium [Ca^{2+}] was stabilized. Then IP_3 was added in increasing concentrations to measure the extent of Ca^{2+} release and the potency of IP_3 in mobilizing Ca^{2+} from the ER.

Measurement of IP_3 mass

IP_3 levels were measured by a radioligand assay (Xu et al., 1996b). Intact acini were stimulated with the indicated concentration of agonist for 5 s at 37°C. Permeabilized acini were stimulated with 2.5–100 μM GTPγS for 15 s at 37°C. Preliminary experiments showed that 1,4,5 IP_3 reached maximal level at these incubation times. The reactions were stopped by the addition of 100 μl ice-cold 15% PCA to 100 μl of samples, vigorous mixing, and incubation on ice for at least 10 min to allow precipitation of proteins. Standards of IP_3 were prepared in the same manner. The perchloric acid was removed, and IP_3 was extracted with 0.2 ml Freon and 0.2 ml tri-*n*-octylamine. IP_3 content in the aqueous phase was measured by displacement of [^{3}H]IP_3 using microsomes prepared from bovine brain cerebella.

Western blot

Microsomes were prepared by homogenizing pancreatic acini or brains from WT, Homer2$^{-/-}$, and Homer3$^{-/-}$ mice in a buffer containing (mM): 100 KCl , 20 Tris-base, pH 7.6 with KOH, 1 EDTA, 1 benzamidine, and 1 PMSF. The homogenates were centrifuged at 1,000 *g* for 10 min at 4°C. The supernatants were collected and centrifuged at 40,000 *g* for 30 min. The pellets were resuspended in homogenization buffer and the microsomes were stored at −80°C until use. Microsomes were extracted by a 1-h incubation on ice in a buffer containing (mM): 50 Tris, pH 6.8 with HCl, 150 NaCl, 2 EDTA, 2 EGTA, and 1% Triton X-100 supplemented with protease inhibitors (0.2 mM PMSF, 10 μg/ml leupeptin, 15 μg/ml aprotinin, and 1 mM benzamidine). The extracts were used to separate the proteins by SDS-PAGE and the proteins were probed with a 1:500 dilution of SERCA2b pAb; 1:500 dilution of IP_3R1 pAb; and 1:1,000 dilution of IP_3R3 and PMCA mAbs.

Pull-down assay

Rat pancreatic acini were used to prepare extracts as described above. Adult rat forebrain was sonicated in four volumes of ice cold PBS with 1% Triton X-100. Soluble extracts were mixed with GST-Homer proteins lined to glutathione beads (Sigma-Aldrich) for 2 h (pancreas) or overnight (brain) at 4°C. Beads were pelleted and washed four times in lysis buffer and eluted with loading buffer followed by SDS-PAGE. The blots were probed for PLCβ, mGlu5α, or stained with Coomassie blue as before (Tu et al., 1998; Xiao et al., 2000).

Immunocytochemistry

Cells from WT, Homer2$^{-/-}$, and Homer3$^{-/-}$ mice attached to glass coverslips were fixed and permeabilized with 0.5 ml of cold methanol for 10 min at −20°C, except for the experiments in Figs. 2 and 4 for localization of Homer 3, in which the cells were fixed with 4% formaldehyde for 20 min at room temperature, followed by permeabilization with 0.05% Triton X-100. After removal of methanol or Triton X-100, the cells were washed with PBS and incubated in 0.5 ml PBS containing 50 mM glycine for 10 min at room temperature. This buffer was aspirated and the nonspecific sites were blocked by a 1-h incubation at room temperature with 0.25 ml PBS containing 5% goat serum, 1% BSA, and 0.1% gelatin (blocking medium). The medium was aspirated and replaced with 50 μl of blocking medium containing control serum or a 1:50 dilution of pAbs against Homer 1, 2, or 3, or a 1:100 dilution of pAb against IP_3R1, 2, or 3. After incubation with the primary antibodies overnight at 4°C and three washes with the incubation buffer (same as blocking buffer, but without serum), the antibodies were detected with goat anti–rabbit or anti–mouse IgG tagged with fluorescein or rhodamine. Images were collected with a confocal microscope (model MRC 1024; Bio-Rad Laboratories).

Measurement of GTPase and PLC activities in vitro

Agonist-stimulated steady-state GTP hydrolysis was measured in reconstituted vesicles that contained recombinant, purified heterotrimeric Gq and M1 acetylcholine receptors at 30°C in the presence and absence of 2–5 nM RGS4 or PLCβ1 (Biddlecome et al., 1996). Homers 1 and 2 (250 nM) were preincubated with the vesicles in the presence of 1 mM carbachol and one of the GAPs for 45 min at 0°C followed by further incubation for 2 min at 30°C (Mukhopadhyay and Ross, 1999). The GTPase reaction was initiated by adding 3 μM γ-[^{32}P]GTP and was continued for 10 min at 30°C. Reactions were quenched with a cold slurry of Norit in H_3PO_4 and [^{32}P]Pi was measured in the supernatant.

The effect of Homer 2 on steady-state phospholipase activity of PLCβ1 was measured with the same reconstituted phospholipid vesicles, which also contained [^{3}H]PIP_2. Homer 2 was preincubated with PLCβ1 for 45 min at 0°C. PIP_2 hydrolysis was initiated by adding a mixture of the preincubated Homer 2 (250 nM final) and PLCβ1 (2 nM final) to the reconstituted vesicles. [^{3}H]IP_3 release was measured at 30°C in the presence of 1 mM carbachol, 10 μM GTP, and 10 nM-free Ca^{2+} as described previously (Biddlecome et al., 1996).

Statistics

When appropriate, results are given as the mean ± SEM of the indicated number of experiments. Statistical significance was evaluated by a two-way ANOVA. All immunostaining experiments were repeated at least five times with similar results.

We thank Jin Chen for superb technical assistance and Daniella Muallem for help in editing the manuscript.

This work was supported by grants from the National Institute of Diabetes and Digestive and Kidney Diseases, the National Institute on Deafness and Other Communication Disorders, the National Institute of General Medical Sciences, the National Institute of Drug Abuse, and the National Institute of Mental Health. Support was also provided by a Korea Research Foundation Grant (KRF-2002-015-EP0115) to D.M. Shin.

Submitted: 21 October 2002
Revised: 16 May 2003
Accepted: 23 May 2003

References

Berridge, M.J. 1993. Inositol trisphosphate and calcium signaling. *Nature.* 361: 315–325.

Biddlecome, G.H., G. Berstein, and E.M. Ross. 1996. Regulation of PLCβ1 by Gq and m1 muscarinic cholinergic receptor. Steady-state balance of receptor-mediated activation and GTPase-activating protein-promoted deactivation. *J. Biol. Chem.* 271:7999–8007.

Brini, M., D. Bano, S. Manni, R. Rizzuto, and E. Carafoli. 2000. Effects of PMCA and SERCA pump overexpression on the kinetics of cell Ca^{2+} signalling. *EMBO J.* 19:4926–4935.

Carafoli, E. 2002. Calcium signaling: a tale for all seasons. *Proc. Natl. Acad. Sci. USA.* 99:1115–1122.

Cook, B., M. Bar-Yaacov, H. Cohen Ben-Ami, R.E. Goldstein, Z. Paroush, Z. Selinger, and B. Minke. 2000. Phospholipase C and termination of G-protein-mediated signaling in vivo. *Nat. Cell Biol.* 2:296–301.

Fagni, L., P.F. Worley, and F. Ango. 2002. Homer as both a scaffold and transduction molecule. *Sci. STKE.* RE8.

Gilman, A.G. 1987. G proteins: transducers of receptor-generated signals. *Annu. Rev. Biochem.* 56:615–649.

Gudermann, T., T. Schoneberg, and G. Schultz. 1997. Functional and structural complexity of signal transduction via G-protein-coupled receptors. *Annu. Rev. Neurosci.* 20:399–427.

Hirose, K., S. Kadowaki, M. Tanabe, H. Takeshima, and M. Iino. 1999. Spatiotemporal dynamics of inositol 1,4,5-trisphosphate that underlies complex Ca^{2+} mobilization patterns. *Science.* 284:1527–1530.

Hering, H., and M. Sheng. 2001. Dendritic spines: structure, dynamics and regulation. *Nat. Rev. Neurosci.* 2:880–888.

Hunter, T. 2000. Signaling—2000 and beyond. *Cell.* 100: 113–127.

Kasai, H., Y.X. Li, and Y. Miyashita. 1993. Subcellular distribution of Ca^{2+} release channels underlying Ca^{2+} waves and oscillations in exocrine pancreas. *Cell.* 74:669–677.

Kiselyov, K., D.M. Shin, and S. Muallem. 2003. Signalling specificity in GPCR-dependent Ca^{2+} signalling. *Cell. Signal.* 15:243–253.

Lee, M.G., X. Xu, W. Zeng, J. Diaz, T. H. Kuo, F. Wuytack, L. Racymaekers, and S. Muallem. 1997a. Polarized expression of Ca^{2+} pumps in pancreatic and salivary gland cells. Role in initiation and propagation of $[Ca^{2+}]_i$ waves. *J. Biol. Chem.* 272:15771–15776.

Lee, M.G., X. Xu, W. Zeng, J. Diaz, R.J. Wojcikiewicz, T.H. Kuo, F. Wuytack, L. Racymaekers, and S. Muallem. 1997b. Polarized expression of Ca^{2+} channels in pancreatic and salivary gland cells. Correlation with initiation and propagation of $[Ca^{2+}]_i$ waves. *J. Biol. Chem.* 272:15765–15770.

Liu, B.F., X. Xu, F. Fridman, S. Muallem, and T.H. Kuo. 1996. Consequences of functional expression of the plasma membrane Ca^{2+} pump isoform 1a. *J. Biol. Chem.* 271:5536–5544.

Luo, X., S. Popov, A.K. Bera, T.M. Wilkie, and S. Muallem. 2001. RGS proteins provide biochemical control of agonist-evoked $[Ca^{2+}]_i$ oscillations. *Mol. Cell.* 7:651–660.

Minke, B., and B. Cook. 2002. TRP channel proteins and signal transduction. *Physiol. Rev.* 82:429–472.

Missiaen, L., H. De Smedt, G. Droogmans, and R. Casteels. 1992. Ca^{2+} release induced by inositol 1,4,5-trisphosphate is a steady-state phenomenon controlled by luminal Ca^{2+} in permeabilized cells. *Nature.* 357:599–602.

Mukhopadhyay, S., and E.M. Ross. 1999. Rapid GTP binding and hydrolysis by Gq promoted by receptor and GTPase-activating proteins. *Proc. Natl. Acad. Sci. USA.* 96:9539–9544.

Nash, M.S., K.W. Young, R.A. Challiss, and S.R. Nahorski. 2001. Intracellular signaling. Receptor-specific messenger oscillations. *Nature.* 413:381–382.

Petersen, O.H., C.C. Petersen, and H. Kasai. 1994. Calcium and hormone action. *Annu. Rev. Physiol.* 56:297–319.

Ross, E.M. 1995. G protein GTPase-activating proteins: regulation of speed, amplitude, and signaling selectivity. *Recent Prog. Horm. Res.* 50:207–221.

Ross, E.M., and T.M. Wilkie. 2000. GTPase-activating proteins for heterotrimeric G proteins: regulators of G protein signaling (RGS) and RGS-like proteins. *Annu. Rev. Biochem.* 69:795–827.

Shin, D.M., X. Luo, T.M. Wilkie, L.J. Miller, A.B. Peck, M.G. Humphreys-Beher, and S. Muallem. 2001. Polarized expression of G protein-coupled receptors and an all-or-none discharge of Ca^{2+} pools at initiation sites of $[Ca^{2+}]_i$ waves in polarized exocrine cells. *J. Biol. Chem.* 276:44146–44156.

Smith, F.D., and J.D. Scott. 2002. Signaling complexes: junctions on the intracellular information super highway. *Curr. Biol.* 12:R32–R40.

Thrower, E.C., R.E. Hagar, and B.E. Ehrlich. 2001. Regulation of $Ins(1,4,5)P_3$ receptor isoforms by endogenous modulators. *Trends Pharmacol. Sci.* 22:580–586.

Tu, J.C., B. Xiao, J.P. Yuan, A.A. Lanahan, K. Leoffert, M. Li, D.J. Linden, and P.F. Worley. 1998. Homer binds a novel proline-rich motif and links group 1 metabotropic glutamate receptors with IP_3 receptors. *Neuron.* 21:717–726.

Xiao, B., J.C. Tu, R.S. Petralia, J.P. Yuan, A. Doan, C.D. Breder, A. Ruggiero, A.A. Lanahan, R.J. Wenthold, and P.F. Worley. 1998. Homer regulates the association of group 1 metabotropic glutamate receptors with multivalent complexes of homer-related, synaptic proteins. *Neuron.* 21:707–716.

Xiao, B., J.C. Tu, and P.F. Worley. 2000. Homer: a link between neural activity and glutamate receptor function. *Curr. Opin. Neurobiol.* 10:370–374.

Xu, X., W. Zeng, J. Diaz, and S. Muallem. 1996a. Spatial compartmentalization of Ca^{2+} signaling complexes in pancreatic acini. *J. Biol. Chem.* 271:24684–24690.

Xu, X., W. Zeng, and S. Muallem. 1996b. Regulation of the inositol 1,4,5-trisphosphate-activated Ca^{2+} channel by activation of G proteins. *J. Biol. Chem.* 271:11737–11744.

Xu, X., W. Zeng, S. Popov, D.M. Berman, I. Davignon, K. Yu, D. Yowe, S. Offermanns, S. Muallem, and T.M. Wilkie. 1999. RGS proteins determine signaling specificity of Gq-coupled receptors. *J. Biol. Chem.* 274:3549–3556.

Zeng, W., X. Xu, and S. Muallem. 1996. $G\beta\gamma$ transduces $[Ca^{2+}]_i$ oscillations and $G\alpha q$ a sustained response during stimulation of pancreatic acinar cells with $[Ca^{2+}]_i$-mobilizing agonists. *J. Biol. Chem.* 271:18520–18526.

Zeng, W., X. Xu, S. Popov, S. Mukhopadhyay, P. Chidiac, J. Swistok, W. Danho, K.A. Yagaloff, S.L. Fisher, E.M. Ross, et al. 1998. The N-terminal domain of RGS4 confers receptor-selective inhibition of G protein signaling. *J. Biol. Chem.* 273:34687–34690.

Zhao, X.S., D.M. Shin, L.H. Liu, G.E. Shull, and S. Muallem. 2001. Plasticity and adaptation of Ca^{2+} signaling and Ca^{2+}-dependent exocytosis in $SERCA2^{+/-}$ mice. *EMBO J.* 20:2680–2689.